

ISSN 0280-5316
ISRN LUTFD2/TFRT--5849--SE

Identification and Modeling of Sensory Feedback Processing in a Brain System for Voluntary Movement Control

Per-Ola Forsberg

Department of Automatic Control
Lund University
February 2010

Lund University Department of Automatic Control Box 118 SE-221 00 Lund Sweden		<i>Document name</i> MASTER THESIS	
		<i>Date of issue</i> February 2010	
		<i>Document Number</i> CODEN LUTFD2/TFRT--5849--SE	
<i>Author(s)</i> Per-Ola Forsberg		<i>Supervisor</i> Henrik Jörntell Dept.of Cerebellar Physiology, BMC, Lund Rolf Johansson Automatic Control, Lund. (Examiner)	
		<i>Sponsoring organization</i>	
<i>Title and subtitle</i> Identification and Modeling of Sensory Feedback Processing in a Brain System for Voluntary Movement Control. (Identifiering och modellering av sensorisk återkoppling i en hjärnstruktur för frivillig rörelsekontroll)			
<i>Abstract</i> <p>The body shows impressive control capabilities in terms of the speed and the precision with which movements can be carried out under a wide variety of circumstances. The cerebellum and brainstem nuclei, including the cuneate nucleus, are believed to play a crucial role in this control. If these control mechanisms can be unveiled, this could yield important insights in not only medicine and neurophysiology, but could also control theory in general, which could then potentially be applied in a variety of industry-based control applications. In this thesis system identification and modeling of one subsystem is considered: the cuneate nucleus. The aim of this project is to create a quantitative model for control of a network of neurons in this structure and to create a detailed single-cell model of the cuneate neuron. A two-pronged approach is used to study the function of this structure. First a black-box like system identification using Matlab with experimental data as in- and output signals is considered. Then, building on a previously developed Scicos neuron model, a detailed neuron model of one cuneate neuron is developed, incorporating many aspects of recently described cellular neurophysiology. Our findings suggest that the cuneate nucleus acts as filter for its input sensory signal, applying a differentiating and phase-lead effect on the transmitted signal. These are interesting features of a control system, and could help understand how the body can attain such a high degree of precision in its movements.</p>			
<i>Keywords</i>			
<i>Classification system and/or index terms (if any)</i>			
<i>Supplementary bibliographical information</i>			
<i>ISSN and key title</i> 0280-5316			<i>ISBN</i>
<i>Language</i> English	<i>Number of pages</i> 43	<i>Recipient's notes</i>	
<i>Security classification</i>			

Contents

1	Introduction	4
1.1	Background	4
1.1.1	Neurophysiology	4
1.1.2	Modeling	6
1.1.3	MATLAB	6
1.1.4	SCICOS	6
2	Problem formulation	9
3	Materials & Methods	15
3.1	Matlab modeling	15
3.1.1	Two neuron model: Tactile Stimulation	17
3.1.2	Two neuron model: Electrical Stimulation	17
3.1.3	Three neuron model: Tactile Stimulation	18
3.2	GESS Neuron Model	18
4	Results	21
4.1	Matlab modeling	21
4.1.1	Two Neuron Model: Tactile Stimulation	21
4.1.2	Two Neuron Model: Electrical Stimulation	26
4.1.3	Three Neuron Model: Tactile Stimulation	28
4.2	GESS Neuron Model	31
5	Discussion	36
6	Conclusion	38
A	Modeling details	39

1 Introduction

This thesis is a combined thesis for the 11th semester thesis at the medical program in Lund and the masters thesis for the program for Engineering Physics at Lund Institute of Technology. It has been possible through cooperation between the Medical Faculty at Lund University and the Lund Institute of Technology. More specifically, it has been done at the Section for Neurophysiology, Cerebellum Group and the Department of Automatic Control.

The reason this project was initiated is that Henrik Jörntell, assistant professor in neurophysiology, and Rolf Johansson, professor in automatic control and M.D., have been discussing a cooperation for some time. Henrik and the cerebellum group have a unique understanding of cerebellar neurophysiology and have built up a very detailed database of single-cell neural recordings from many of the important structures related to human movement control, yielding new insight. Rolf Johansson, on the other hand, has vast experience from the field of automatic control in general, and is involved in several other cross-disciplinary research projects in medicine involving system modeling, identification and adaptive control.

1.1 Background

1.1.1 Neurophysiology

The importance of the cerebellum and related brainstem nuclei in motor control has now been known for quite some time, but the exact mechanisms with which this is achieved has only partially and gradually been discovered [1],[2]. The cerebellum can act as part of an adaptive control system, and adaptation is important in many reflexes, such as the ocular reflex [1]. The anatomical structure of the cerebellum [2] and other important structures for motor control, such as the cuneate nucleus, have been revealed with quite some detail, and seem to play a crucial role in motor control. Important features such as modular organization of control circuits, synaptic plasticity, silent synapses and spike discharge patterns have been revealed [1]. It has also been shown that the cerebellum plays important roles in not only controlling motor functions, but in cognitive functions as well [1]. It seems that the cerebellum contains internal models of the motor apparatus, which are used to improve motor control [3]. Models of important control aspects such as stability and motor adaptation exist [4]. Although the computing power has increased dramatically, no artificial control system has been designed that works as flexibly and as robustly as a biological control system, such as motor control [5]. Several modeling techniques exist for spiking neural models such as Hodgkin-Huxley type, integrate-and-fire models, interacting with current-based or conductance-based synapses, using clock-driven or event-driven integration strategies [6], [7].

The cuneate nucleus is one of the dorsal column nuclei. It carries fine touch and proprioceptive information from the upper body to the thalamus and cerebellum via the medial lemniscus [8], [9], [10].

Jörntell and colleagues have done much experimental work on the detailed characteristics of neurons in the cerebellum, which gives a unique opportunity to use this data for system analysis and modeling purposes [11], [12], [13], [14], [15].

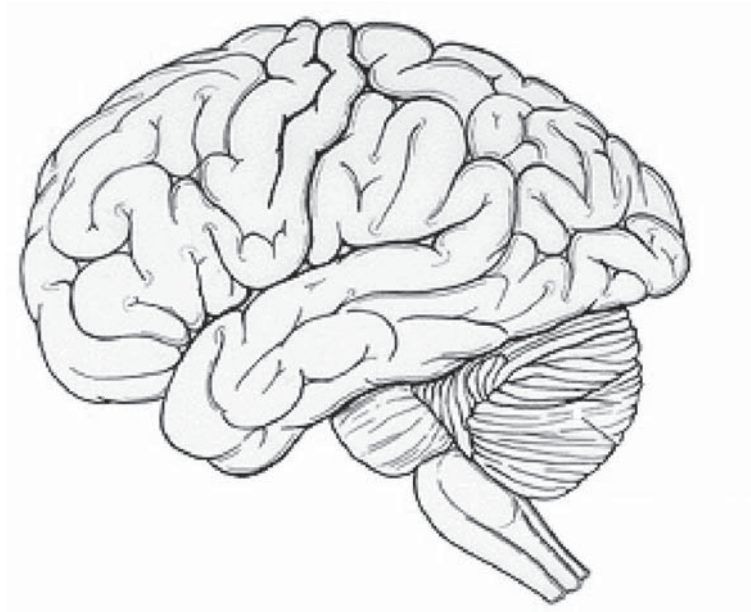


Figure 1: Sketch of the human brain, seen from the left side, with the cerebellum visible at the lower right side. The cuneate nucleus is a small internal structure, not visible on this sketch.

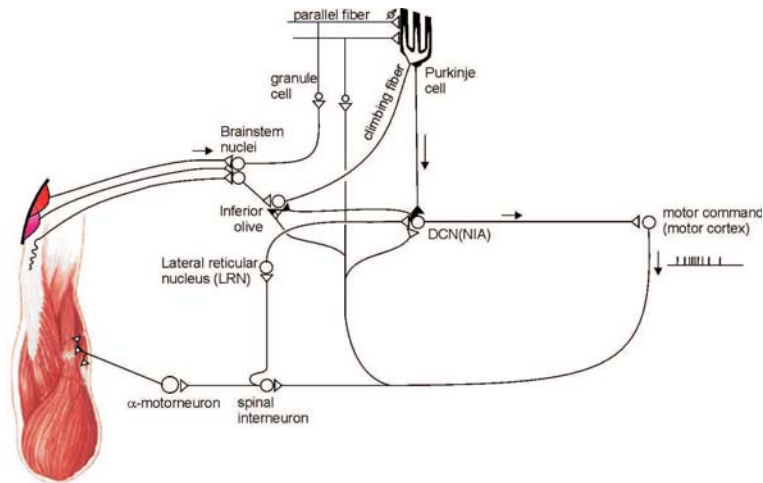


Figure 2: Sketch of how parts of the cerebellum (granule cells, Purkinje cells and Deep Cerebellar Nucleii, DCN), brainstem nuclei (cuneate nucleus) and other structures in nervous system can act as a control system for the motor command acting on a muscle. In reality, each cell connects to a large number (up to 1000) of target cells in a complicated pattern (not showed here).

1.1.2 Modeling

The modeling and identification has run in two parallel tracks for the duration of the project: One track consisted of using experimental data in MATLAB utilizing the System Identification toolbox. The other track used the same experimental data in a generic executable stochastic spiking neuron model (GESS), developed by Martin Nilsson and Henrik Jörntell in Lund in the SCICOSLAB [17] environment.

1.1.3 MATLAB

MATLAB is a numerical computing language developed by THE MATHWORKS, well known in the engineering community. The System Identification Toolbox extends MATLAB for estimating mathematical models to fit measured data. These models might then be used to simulate the output of a system for a given input and to analyze system response, predict future system outputs, or for control design.

A lot of insight into the field of system modeling and identification was given from [16].

1.1.4 SCICOS

SCICOS (Scilab Connected Object Simulator) is a SCILAB package for modeling and simulation of dynamical systems, very similar to MATLAB's Simulink. SCILAB and SCICOS are freeware, however. In this environment, Martin Nilsson and Henrik Jörntell developed GESS (Generic Executable Stochastic Spiking neuron model) in 2008. GESS is released with an OSF modified BSD license, OSF 2008 [18].

GESS was designed to model a single neuron using a number of clock-driven periodical synaptic inputs, integrating them in the soma and then using a stochastic spike firing mechanism in the axon hillock.

For each synapse, a number of constants can be set: gain g , time constant τ and the scaled reverse potential E . Each synapse is driven by a clock, triggering events periodically. These events then generate a square wave of 1 ms duration, considered a normalized action potential. With the neuron membrane potential u , and the membrane time constant T the generated current I for each synapse is then modeled as:

$$I = (u - E) \cdot g \cdot e^{-t/\tau} \cdot \int_0^t e^{t'/\tau} \cdot x/\tau dt' \quad (1)$$

where x is the input signal with normalized action potentials for each triggered event. This is implemented in the model as first applying the low-pass filter, and then calculating the current from the difference between neuron membrane potential and the scaled reverse potential for the synapse major ion type.

For all the synapses, the net current to the soma is calculated by simply adding the individual synapse currents I , with the post-spike current from the firing of that actual neuron (described below). In the soma, current I is con-

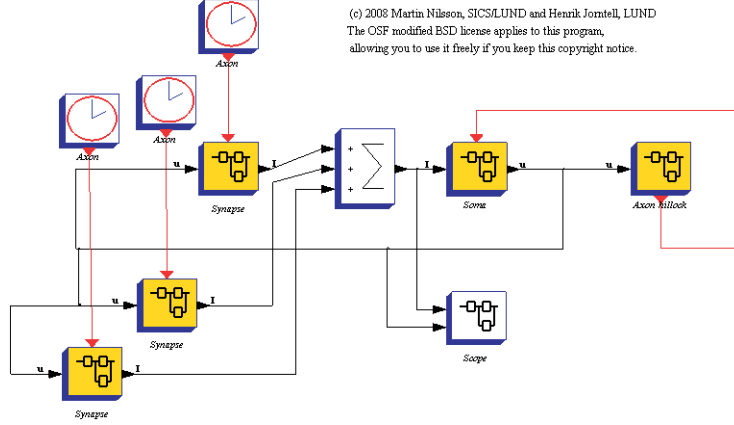


Figure 3: Overview of Gess, 2008 version. The model consists of activating clocks, synapses, soma and an axon hillock super block. GESS is released with an OSF modified BSD license, OSF 2008 [18].

verted to a membrane potential u through

$$u = g \cdot e^{-t/T} \cdot \int_0^t e^{t/T} \cdot I/T dt \quad (2)$$

In the axon hillock, several steps are taken to model the spiking characteristic of the neuron to be considered itself. As for the synapses, a number of constants can be set: α and β (to determine spiking intensity), and the absolute refractory period t_a . The spiking intensity ρ is then given as

$$\rho = \alpha * e^{\beta * u} \quad (3)$$

The cumulative distribution function (CDF) is the given by

$$\frac{dF}{dt} = (1 - F) * \rho \quad (4)$$

This, coupled with a random number generator, then decides when to fire an action potential. In this model, the actual action potential is not modeled, but the trigger event activates a post-spike current in the soma. Here, just as for the synapses, a number of variables can be set: gain g , time constant τ and the scaled reverse potential E . Just as for the upstream synapses, each event triggers the formation of a normalized action potential of 1 ms width, which is then gives the current contribution I from

$$I = (u - E) \cdot g \cdot e^{-t/\tau} \cdot \int_0^t e^{t/\tau} \cdot x/\tau dt \quad (5)$$

which is added with the net current from the upstream synapses.

Then the net current I and membrane potential V is exported to an oscilloscope, where the overall behavior of the neuron can be observed.

This model is a general-neuron model which incorporates many well-known features of neuronal physiology. However, several additions and modifications are necessary for this to be a viable model of a cuneate neuron.

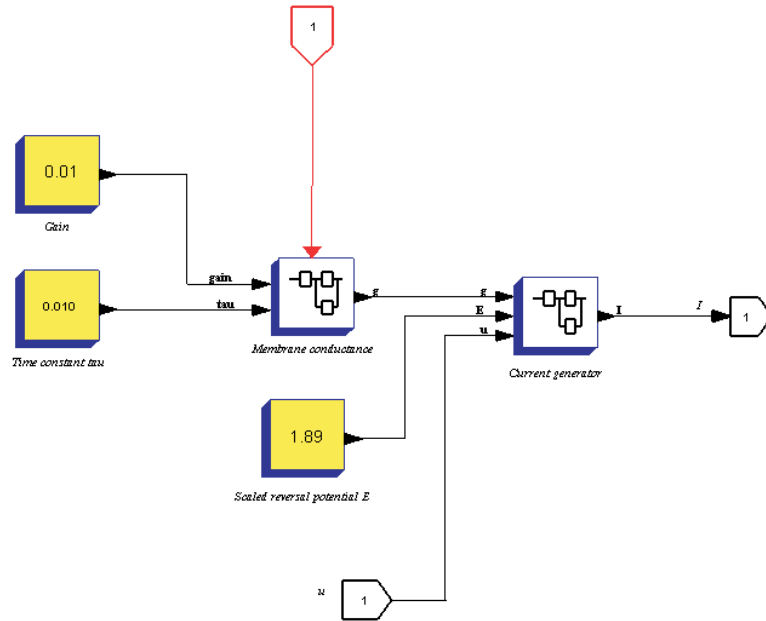


Figure 4: Overview of the synapse superblock, with variable constants in yellow. For each clock-driven event (red 1), a square wave normalized action potential is generated. The incurred current signal is passed on to the soma (black 1).

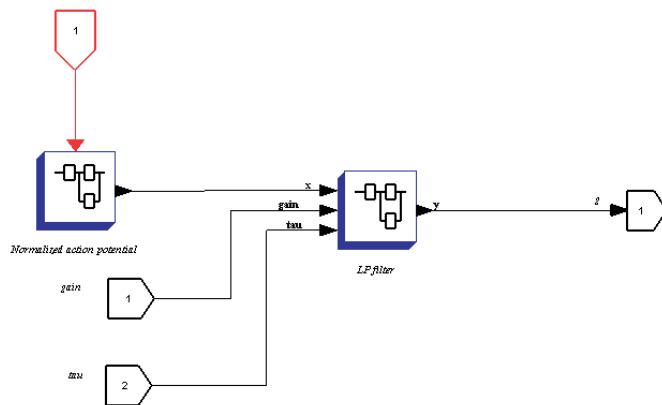


Figure 5: Membrane conductance superblock. Triggering events arrive at (red 1), which produces a normalized action potential in the Normalized action potential superblock. This, together with constants g and τ are then fed to the Low-Pass filter, generating a current I .

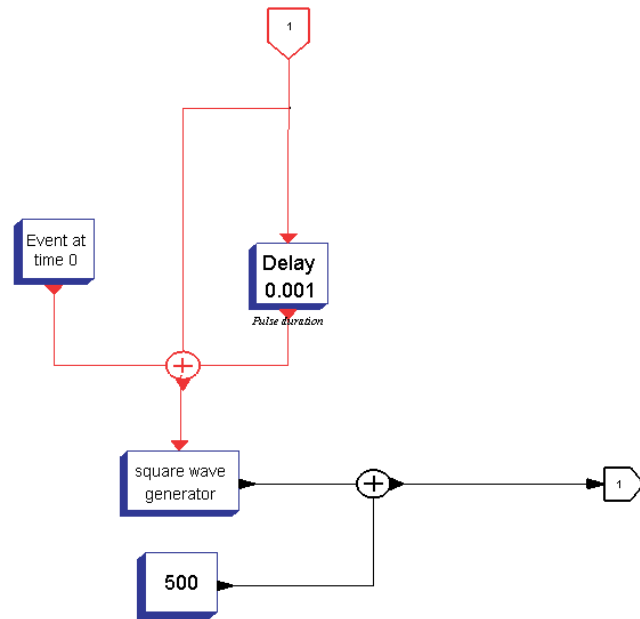


Figure 6: Normalized action potential superblock, which lies in the membrane conductance superblock, inside the synapse superblock. Triggering events arrive at (red 1), which activates a square wave generator block to produce a normalized action potential of 1 ms duration.

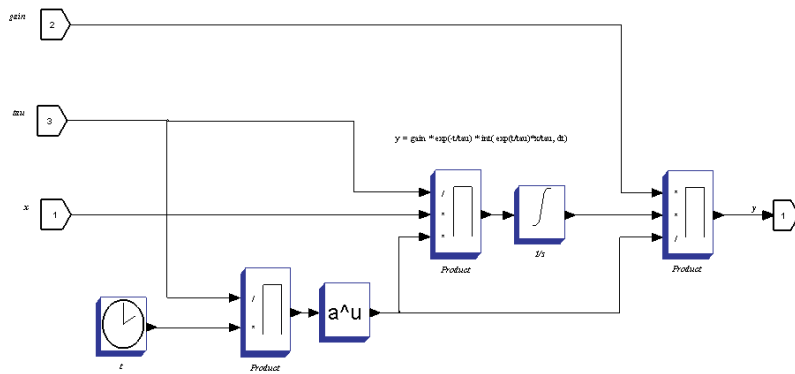


Figure 7: Low-pass filter superblock, which lies in the membrane conductance superblock, inside the synapse superblock. The modulates the incoming signal according to Eq. 7.

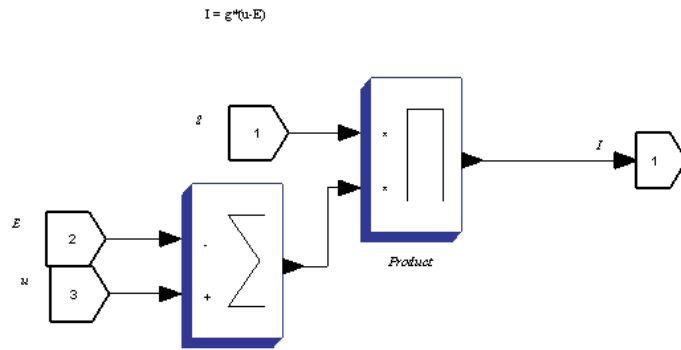


Figure 8: Current generator superblock, which lies in the synapse superblock. The block generates a current I dependent on the gain g , membrane potential u and scaled reversal potential E .

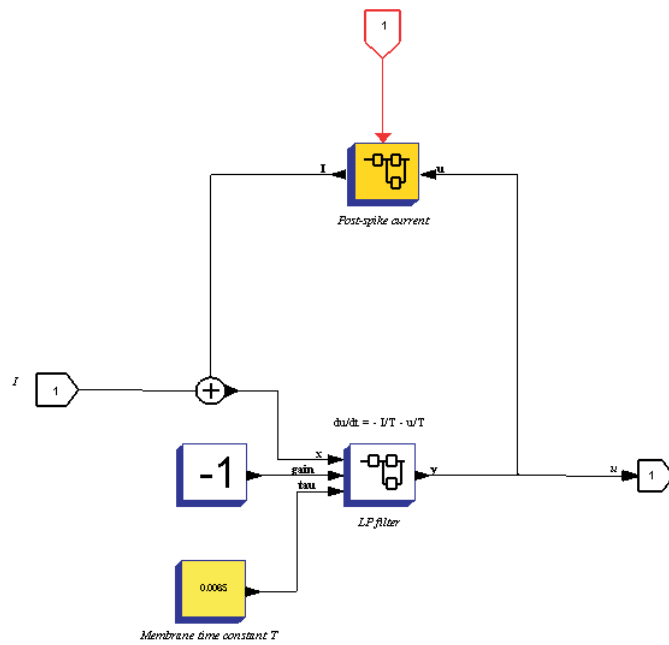


Figure 9: Overview of the soma superblock. Here the synapse currents I (black 1) are added with the post-spike current of the cuneate neuron itself. Events generated by the axon hillock arrive at (red 1). The currents are then transformed to membrane potential in the LP filter superblock, and the net soma membrane potential is then exported as u in (black 1).

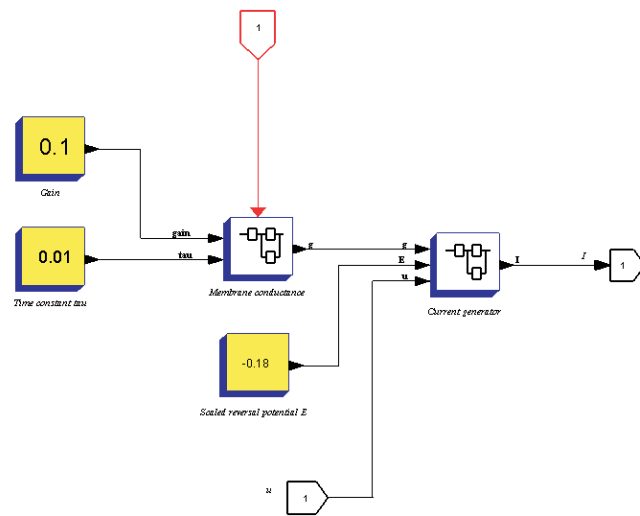


Figure 10: Post-spike current superblock, which lies within the soma superblock. Variable constants in are in yellow. Events generated in the axon hillock superblock arrive at (red 1) to trigger a post-spike membrane conductance change in the membrane conductance superblock. This is then transformed to a current I in the current generator superblock. Membrane conductance and current generator superblocks shown here are identical with Figs 5 and 6, respectively.

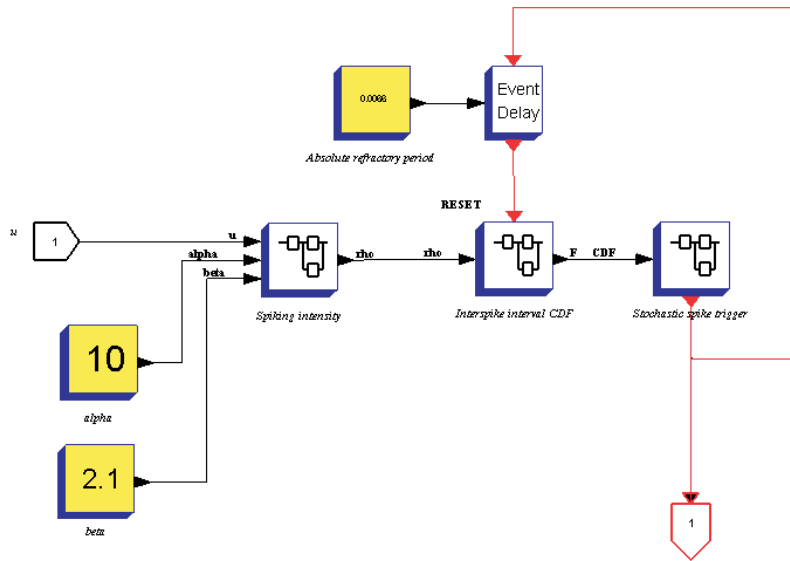


Figure 11: Overview of the axon hillock superblock. α and β are set constants which determine the spiking intensity, in the spiking intensity superblock. An absolute refractory period can also be set, which prevents the neuron from firing continuously. The spike interval is determined in the interspike interval CDF superblock, to which a stochasticity is added in the stochastic spike trigger superblock. This then generates spike events, depending on the membrane potential u , α , β , absolute refractory period and the time after last spike.

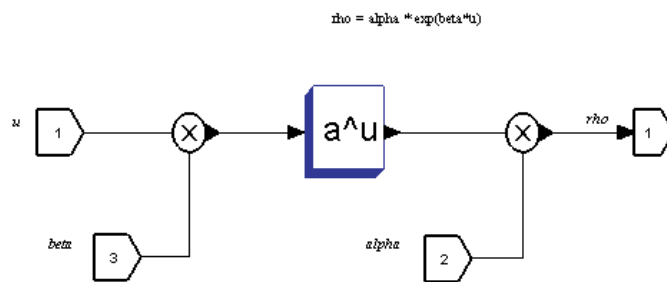


Figure 12: Spiking intensity superblock, which lies within the axon hillock superblock. This block gives the spiking intensity ρ according to Eq. 3.

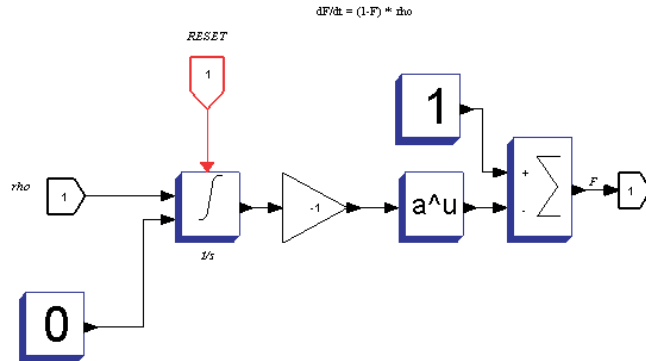


Figure 13: Interspike interval CDF superblock, which lies within the axon hillock superblock. This gives the cumulative distribution function (CDF) according to Eq. 4.

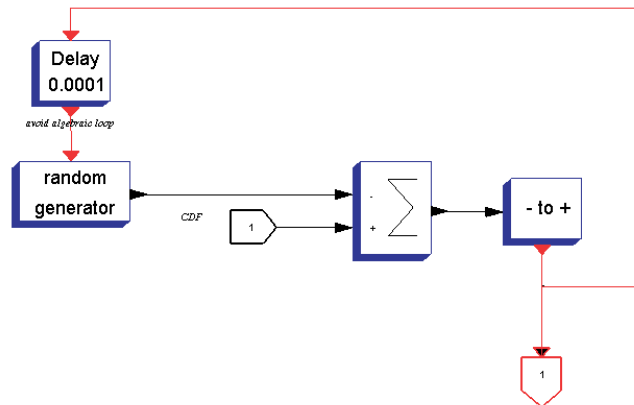


Figure 14: Stochastic spike trigger superblock, which lies within the axon hillock superblock. Here the cumulative distribution function, CDF, is compared with a random number for each time unit. Whenever $CDF > \text{random number}$, a spike event is triggered, and the random number and CDF are reset.

2 Problem formulation

The aim of this project is to create a quantitative model for control of a network of neurons in the cerebellum and the cuneate nucleus, and to create a detailed single-cell model of the cuneate neuron based on an existing GESS model. This will be done using experimental data from ongoing work by the Jörintell group on the behavior of individual neurons in response to different stimuli.

3 Materials & Methods

The modeling and analysis work was made based on experimental data previously collected by the Jörntell group. The experiments were carried out with single unit metal microelectrodes and whole cell patch clamp recordings in the acute animal preparation of the decerebrated cat. Primary afferent axons were recorded on their pathway into the cuneate nucleus and cuneate neurons were recorded inside the cuneate nucleus, see Fig. 15. Stimuli were delivered in two different ways. The first, which was used to produce the model through the system identification, was a standardized manual skin stimulation. A miniature strain gauge device was mounted on the tip of the investigator in order to control that the same amount of force and the same stimulation time was used. A second mode of stimulus was electrical skin stimulation applied through a pair of needle electrodes inserted into the skin with a spacing of 3 mm. Stimulation intensity was 1.0 mA, duration 0.1 ms. All experimental settings and procedures are similar to those in [11].

In order to understand the procedure and the experimental setup, I participated in a few experiments.

3.1 Matlab modeling

This section describes modeling of the first system to be considered, which consists of a number of primary afferent neurons projecting to a single projection neuron in the cuneate nucleus. Experimental data consists for this system for four different experimental setups: 1) No stimulation (background data) 2) Light touch stimulation 3) Airpuff stimulation and 4) Electrical stimulation. The experiments are made in a way such that the receptive field on the cat digit is stimulated by the stimulus mentioned above for a large number (30-40 for light touch, 280 for electrical stimulation) of consecutive stimulations. An electrode is at the same time in place for the primary afferent recording in close vicinity of the primary afferent neuron in the cuneate nucleus. For the cuneate neuron recording, the electrode is in close vicinity of the cuneate neuron in the cuneate nucleus. The recordings of different neurons are not simultaneously done, since the experimental setup does not allow for this. This leads to a problem of causality: How do we know that the signal transmitted by the primary afferent is the one affecting the cuneate nucleus we're observing?

This problem can be alleviated by the fact that the cuneate nucleus has a very high degree of spatial organisation, and the fact that the two different recordings (of the primary afferent and the cuneate neuron) are made very close to each other (in the scale of hundreds of micrometers). Another problem arises: How can we relate input-output data if the experimental triggering is different? (Due to different experiments). This is accomplished by conducting the experiments and stimulations in a standardized way: for both the primary afferent recording and the cuneate neuron recording the tactile and electrical stimulations are made in a standardized way. However, this standardization is not perfect due to the tactile stimulation being "hand-made", why we need to select a number of stimulations for both setups that are as similar as possible. This is possible as the tactile stimulation strength and duration is recorded and controlled for.

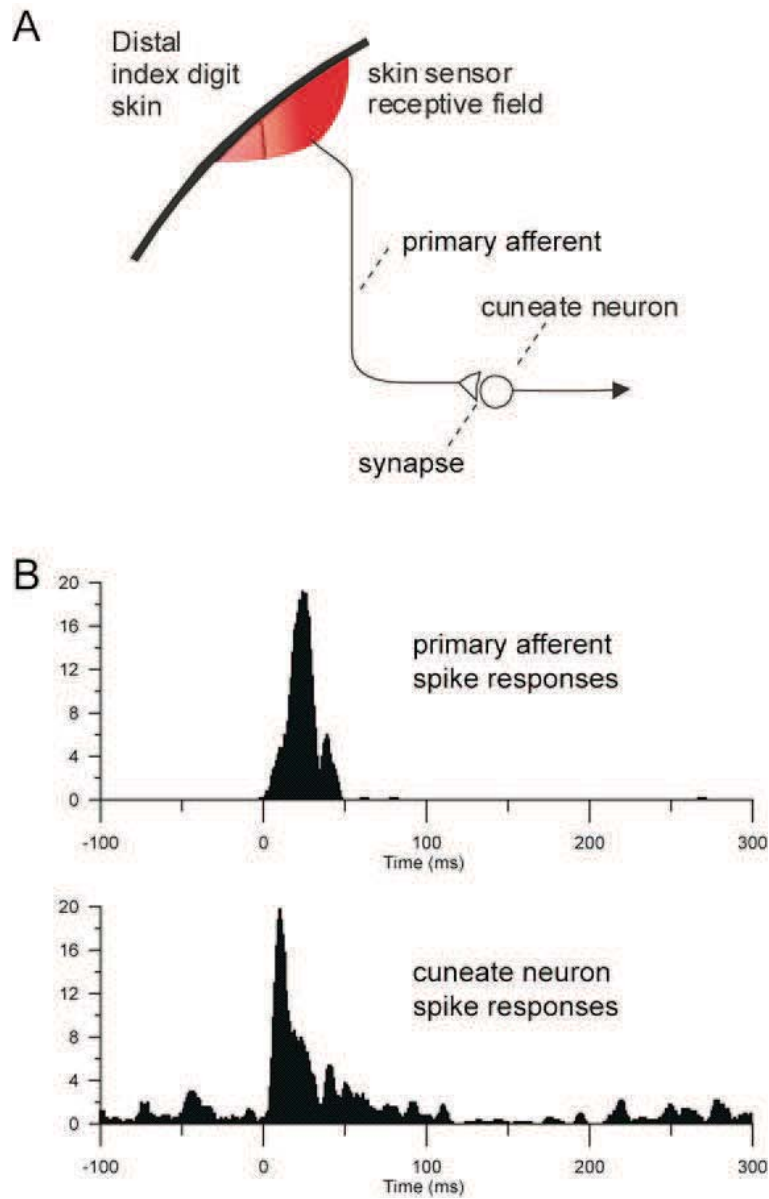


Figure 15: (A) Overview of the experimental setup. Cuneate neurons receive input from primary afferents, which in turn are excited from peripheral receptors (in this case the skin of the distal index finger or digit) and make excitatory synapses on the cuneate neuron. (B) Using the same, standardized manual skin stimulation, data for the spike responses evoked in the primary afferents and cuneate neurons were stored as peristimulus histograms (bin width 1 ms, stimulation started at time 0). The duration of each stimuli in this case was indicated to be 50 ms by the strain gauge device.

The first attempt of modeling this was done using raw voltage-time-data recordings. This was however very difficult to work with, as the signal-to-noise ratio of the evoked versus the spontaneous spiking activity of the neuron was very unfavorable and as the modeling techniques used were not able to capture the fast dynamics of the action potentials (spikes).

3.1.1 Two neuron model: Tactile Stimulation

The two neuron model consists of one primary afferent neuron transmitting sensory information projecting on one cuneate neuron. In reality, however, up to 1000 primary afferents synapse on one cuneate neuron, each sending spike data. Ongoing work indicates that a majority of these inputs have very weak synaptic connectivity/weight, leading to only a few being really relevant for signal transmission to each cuneate neuron (this is believed to be done through learning processes). In this thesis this problem is alleviated by the fact that raw data is not used, but rather spike-time histograms, in effect adding up the contribution from many primary efferent neurons for one stimulation.

The raw data carrying near-identical inputs from neuron recordings in the form of time-voltage series for the consecutive stimulations is processed before applying the system identification tools in the following ways: First the appropriate (congruent) stimuli are selected, and a time-window of 300 ms from start of stimuli is selected. In a separate analysis software, an action-potential pattern identification tool is then used to determine the time at which each action potential is detected after the start of the stimulus. After this, the spike-time data after stimulation is superposed for a number of experiments (45 for the primary afferent and 39 for the cuneate neuron, for tactile stimulation) to create spike-time histograms of bin size 1 ms. Also, to compensate for a limited number of experiments a model is made where each bin data is averaged over 5 bins to smooth the edges.

This data, in the form of two arrays of spike-time histograms, was imported in MATLAB for different setups: 1) starting with the start of the stimulus and 2) starting the recording 100ms before the start of the stimulus in order to allow the transition between the spontaneous and evoked activity to form part of the model properties. Also, the two different forms (the histograms and the over 5 bins averaged histograms) were imported. The input-output relationship of this system (one input and one output) was analyzed using the System Identification Toolbox. For the tactile stimulation, six model classes were evaluated: 1) Prediction error estimate (PEM) 2) ARX 3) ARMAX 4) Output Error 5) Box-Jenkins and 6) State-space model using sub-space method (N4SID). See [16] and [19] for details on the model types. This was done for different sets of experimental data. Model orders were determined based on which gave the best overall fit.

3.1.2 Two neuron model: Electrical Stimulation

The next experimental setup to be analyzed was the electrical stimulation. This gives a very short (<0.1 ms) electrical stimulation of the same skin region analyzed previously, for the light touch stimulation, for 280 consecutive stimulations. This is a very standardized stimulation. It can be seen as the impulse

response of the system. However, the impulse response of the models based on tactile stimulation will not be directly transferrable to the electrical stimulation setup, as we will see later. When modeling this, the primary afferent, initially input data was modeled directly as a spike histogram with a 280 spike amplitude at 4 ms after stimulation (due to conductance delay). As the cuneate nucleus fires briefly in response to this stimulation, but with a very high frequency (>1000 Hz), modeling was also done with 0.1 ms bin width. For both these setups, experimental data for the cuneate neuron was used. Modeling the primary afferent neuron firing as a spike histogram with only one bin of 280 spike amplitude might be accurate when having 1 ms bin width (though it's more likely spread over 2-3 ms), but it does not reflect reality for 0.1 ms bin width.

3.1.3 Three neuron model: Tactile Stimulation

The first simple two neuron network consisted of a primary afferent neuron transmitting sensory data from the forelimb to a cuneate neuron in the cuneate nucleus. It is known that another type of neuron plays an important role in this transmission: the inhibitory interneuron. The primary afferent neuron activates both the cuneate and the inhibitory neuron. Then the interneuron inhibits the cuneate neuron in a feed-forward inhibition arrangement. This thus forms a three neuron network, with one input (the primary afferent axon) and one output (the cuneate neuron axon), see Fig. 16. In reality, each neuron in this circuit makes synapses with many different target neurons. But as for the two neuron model, we come around this using histogram data, leading to a simplified circuit of only three cells.

The first attempt to model this used a two input (primary afferent and interneuron) two output (cuneate neuron and interneuron) MATLAB model. This, however, did not yield meaningful results as it does not reflect the anatomical and neurophysiological structure of the cuneate nucleus, so the model was limited to a two input (primary afferent and inhibitory interneuron) one output (cuneate neuron) system. The data used was the same light touch stimulation data used for the two neuron circuit for the primary afferent and the cuneate neuron. For the inhibitory interneuron, only light touch data for a slightly longer stimulations (70 ms) and for 6 consecutive stimulations only was available (added, as for the other data, into a spike-time histogram), as seen in Fig. 27.

3.2 GESS Neuron Model

In order to make a detailed and accurate model of the cuneate neuron using the existing GESS model, described in the introduction, a large number of modifications needed to be made.

First, the clock-driven events activating the synapses was changed into a module which could read real experimental data, in order to use the data collected by Jörntell and colleagues. The data itself was also on a form not recognizable by the SCILAB environment, and was thus processed to be so. Here spike-time data is used recorded from single tactile stimulations, as opposed to the spike-time histograms used in the MATLAB modeling, due to the fact that we want to build an as accurate model of the actual single neurons as possible.

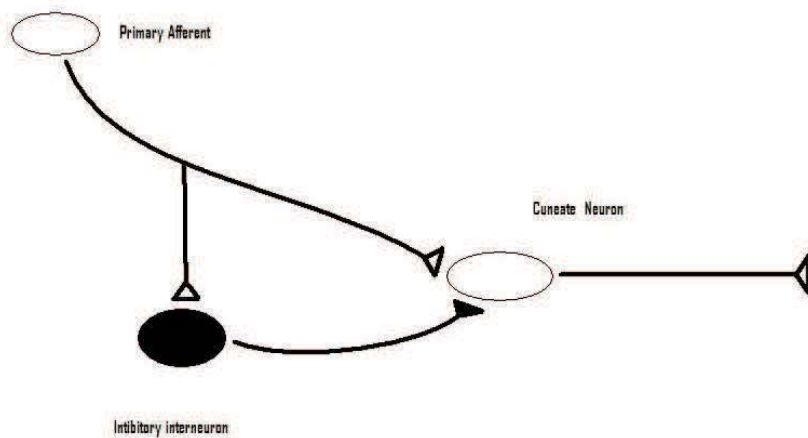


Figure 16: Sketch of the 3 neuron model. Skin stimulation activates the primary afferent neuron, which makes excitatory synapses with the cuneate neuron, as well as with interneurons in the cuneate nucleus. The interneuron then makes an inhibitory synapse with the cuneate neuron. In reality, these cells synapse with a large number of target cells each, but for our modeling purpose, we use a simplified version, as the diagram shows.

Then, in order to follow the spiking activity of the model, a module generating action potential spikes was added.

An analysis was made regarding the time-resolution of the model in order to understand whether it was necessary and possible to increase the resolution from 1 ms.

The synapses were then extended to include more excitatory synapses, as well as inhibitory synapses coming from the inhibitory interneurons, for which data was also available. A lower number of synapses was set than is present *in vivo*. This is reasonable, however, as most synapses *in vivo* have very low synapse weights and can thus be ignored.

Experimental data from tactile stimulation was then read as input for each of the synapses, and the model behavior and cuneate neuron firing pattern was observed.

The model parameters (time constants etc.) were estimated based on a number of different scenarios, including activation of one synapse, looking at membrane potential behavior under different circumstances and firing of action potentials/spikes from the axon hillock.

A detailed study of the spiking probability density function, given by Eq. 3, was made, as the spike firing from the model involves some stochasticity. A MATLAB model of this was made to study the behavior, and some work was done to try to understand the dynamics.

Another feature was added to the model both on incoming and outgoing spike firing: Paired Pulse Depression. This means, basically, that when several spikes in a single axon are fired/received by the same synapse, sequential responses of this synapse will show a depression, i.e. the individual synaptic responses have a gradually lower impact on membrane potential than it would have been if they would have had a larger timespan between them. This is observed *in vitro*, and from a neurophysiological point of view, could be explained by e.g. synapse exhaustion.

4 Results

4.1 Matlab modeling

4.1.1 Two Neuron Model: Tactile Stimulation

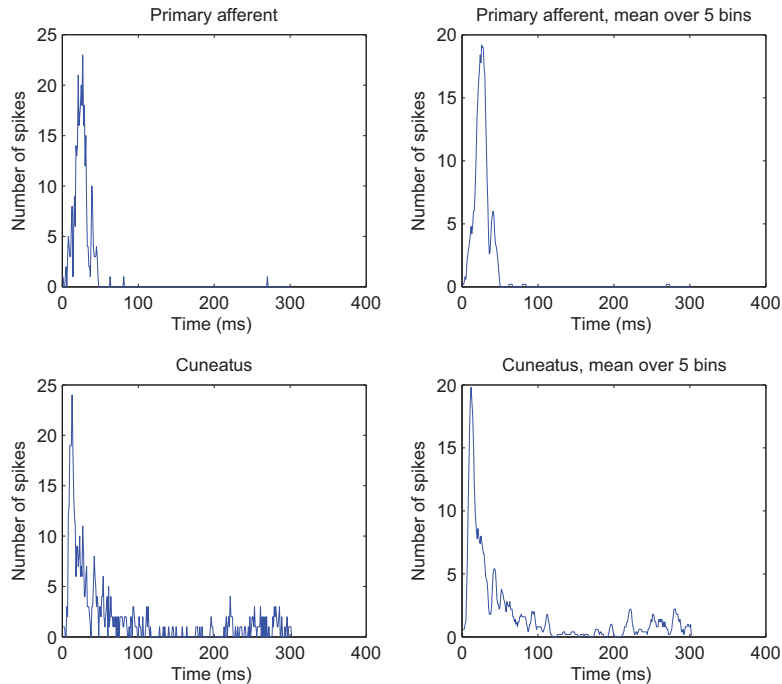


Figure 17: Histogram and averaged-over-5-bins histogram data used for the input (primary afferent neuron) and the output (cuneate neuron) [11]. The tactile stimulation starts at time 0 ms. Data from [11].

Figure 17 shows the experimental histogram data used for the two neuron tactile stimulation model. Figure 18 and Figure 19 show how the different model types (m1-m5) are able to reproduce the output signal (primcun) from the tactile stimulation input signal, for histogram and averaged histogram data, respectively. The models used are, for m1-m5, PEM, ARX, ARMAX, OE and BJ.

The models seem to be much better if only data from the start of the stimulation is considered, rather than including prestimulus. This seems to be due to the fact that the models can't replicate the spontaneous background activity the cuneate neuron shows, which is not seen in the primary afferent input data. Even when considering data from the start of the stimulation only and up to 300 ms after, the models do a good job of following the initial spike train, but fail to capture the spontaneous firing activity which dominates the signal far from the stimulus (near the end of the 300 ms). A reflection here could be that the spontaneous activity of the cuneate neuron likely does not contain any relevant

information for the nervous system. Rather, this could reflect that the cuneate neuron membrane potential always lies very close to the firing potential, in order to be able to start firing very rapidly once it gets input from the primary afferent neurons. However, having a spontaneous firing activity gives the cuneate neuron the possibility to actually decrease it's firing frequency in response to inhibition.

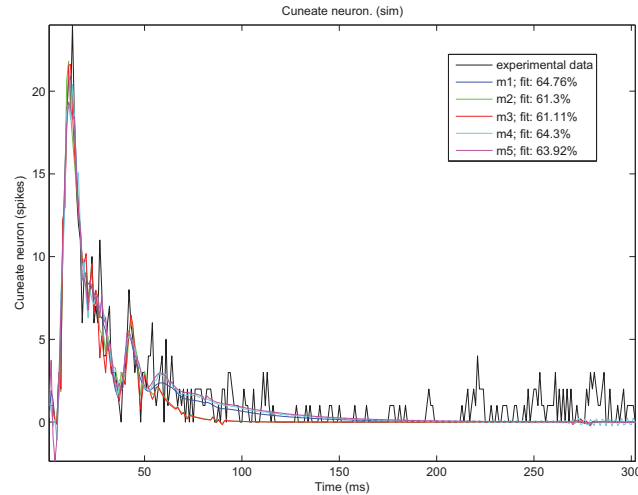


Figure 18: Model ability to predict output spike histogram. Models m1-m5 are PEM, ARX, ARMAX, OE and BJ, respectively. After adjustnig model orders, the model fit ranges between 61-66%. See [16] and [19] for model structures.

What is also apparent from the modeling is that the models fit better to the averaged data. This probably reflects the fact that the data is more smooth, as it does not contain as sharp spikes as the original data. One danger here is, of course, that valuable characteristics of the information processing of the cuneate neurons could be lost.

Another important aspect, that is not taken into consideration here, is that there is one additional neuron type in this circuit: the primary afferent axon also branches off to an inhibitory interneuron, which then inhibits the same cuneate neuron which the primary afferent neuron excites.

Let's consider one model (m1, see appendix A for details), which seems to describe system behavior in a good way, e.g. the PEM-model, starting with the start of the stimulus. Below are the bode and impulse diagrams of m1 (Figs 20 21). A Bode plot is a graph of the transfer function of a system (in this case model m1) versus frequency, to show the system's frequency response. It usually consists of a bode magnitude diagram and a bode phase diagram, which describe how, in this case, the model transforms an oscillating input signal. The impulse response of a system is its output in response to a brief input signal, a spike or impulse. Analyzing Bode diagrams of models can be used to give insight into model behavior. For details on Bode diagrams and impulse-response analysis

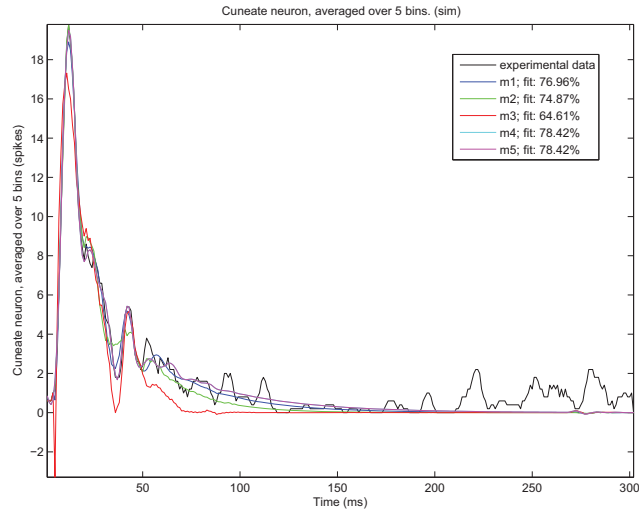


Figure 19: Model ability to predict output spike histogram, averaged over 5 bins. Models m1-m5 are PEM, ARX, ARMAX, OE and BJ, respectively. After adjusting model orders, the model fit ranges between 74-78%. See [16] and [19] for model structures.

see [16].

Fig. 22 shows the zero-pole diagram for PEM model m1. Fig. 23 shows the residual autocorrelation and cross correlation for PEM model m1, with 99%-confidence interval limits for noncorrelated residuals. This indicates that model m1 of order 6 can be accepted.

This model shows some interesting properties. Firstly, one can see that it has deriving properties in a fairly large part of the spectrum. It is worth noting that the firing frequency of the primary afferent neurons never exceeds 500 Hz ($\simeq 10^{-1}$ rad/ms). Speculating, this could have to do with wanting to increase spatial and temporal resolution of the sensory data, which is then transmitted further on in the nervous system. Secondly, the model shows phase lead, which is a very useful property of control systems in order to better predict and maintain good control.

Looking at the impulse response, it is interesting to note that this is a very good match of the output the cuneate nucleus produces in response to an electrical stimulation of the skin - which can be considered an impulse.

However, looking at the other models, the differentiating properties are not prevalent. Phase lead, on the other hand, is present in almost all other models (data not shown).

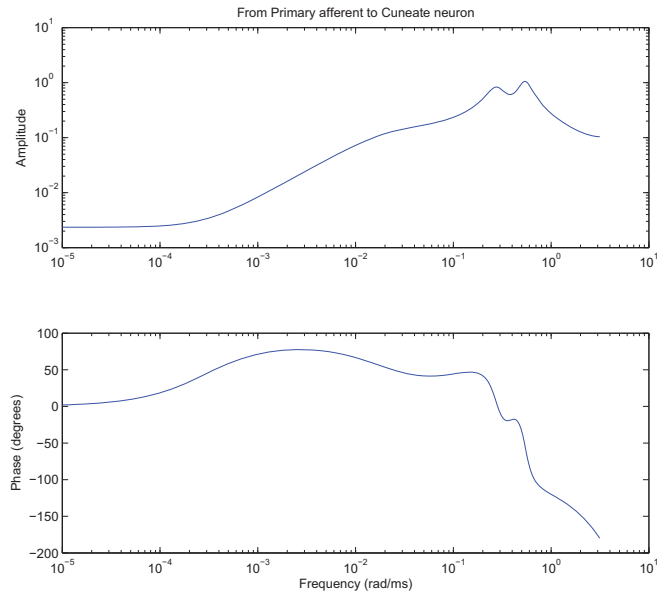


Figure 20: Bode diagram of the PEM model. Notice differentiating and phase lead properties for parts of the spectrum. It is worth noting that the firing frequency of the primary afferent neurons never exceeds 500 Hz ($\approx 10^{-1}$ rad/ms.)

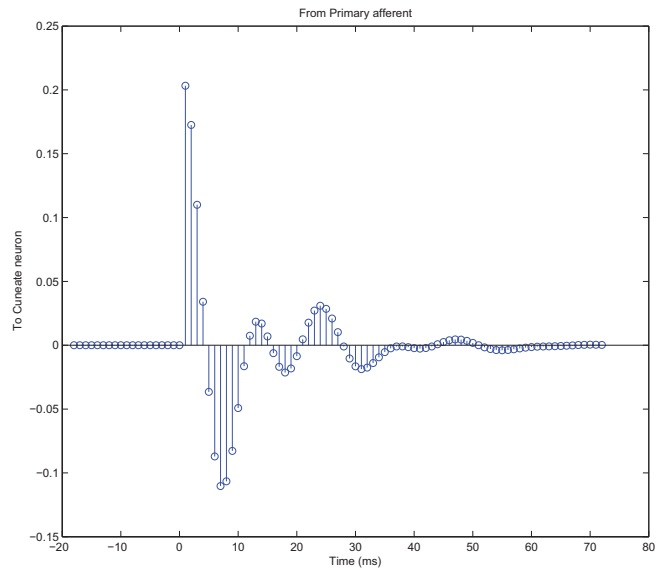


Figure 21: Impulse response for the PEM model m1.

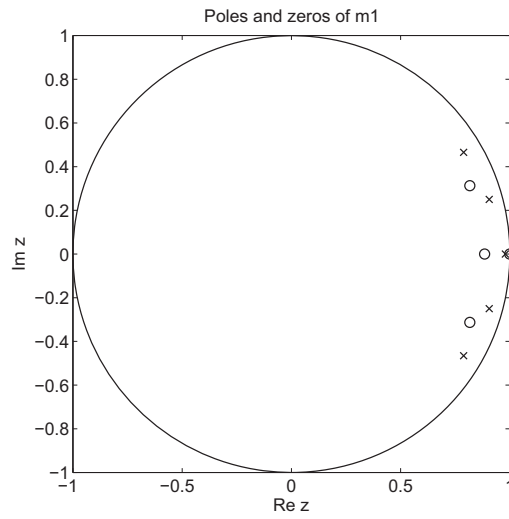


Figure 22: Zero-pole diagram of the PEM model m1 containing poles ('x'), and zeros ('o').

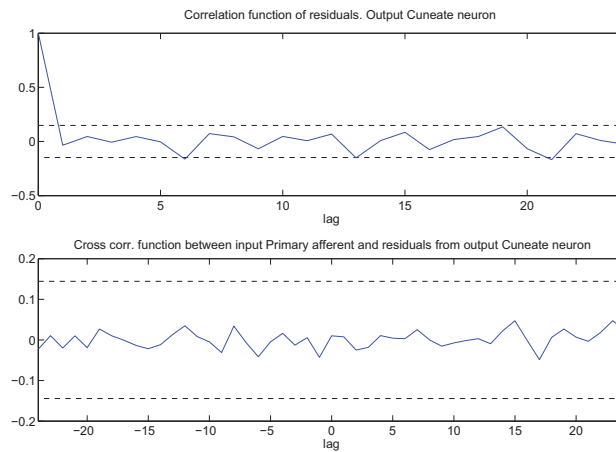


Figure 23: Residual autocorrelation (top) and cross correlation (bottom) for PEM model m1 of order 6 with 99%-confidence interval limits (dashed line) for noncorrelated residuals.

4.1.2 Two Neuron Model: Electrical Stimulation

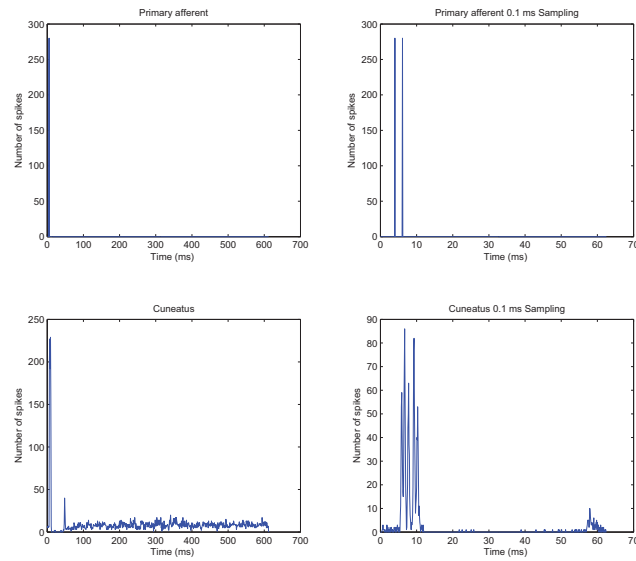


Figure 24: Data used for the electrical stimulation modeling [11]. The left side shows data with 1 ms time resolution. The right side shows data with 0.1 ms time resolution. The top diagrams show cuneate model input histogram data, whereas the lower show cuneate neuron output histogram data, as measured experimentally. Data from [11].

The data used for the modeling is showed in Figure 24. One big advantage of using a high number of stimulations (280), as in the case for the electrical stimulation, is that the background activity and noise has a small impact (Fig. 24).

As seen from the modeling of the 1 ms bin width electrical stimulation in Figure 25, the models can capture these dynamics fairly well (fit ranging from 53.2-80.3%).

When looking at the models for the electrical stimulation with 0.1 ms bin width (Fig. 26), it is evident that the models do a fairly poor job of following the very fast firing pattern of the cuneate neuron in response to the impulse-like stimulation.

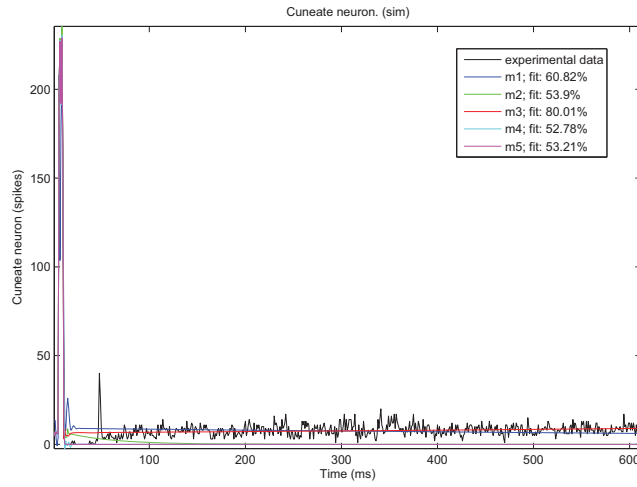


Figure 25: Models for the electrical stimulation for 1 ms bin width. Models m1-m5 are PEM, ARX, ARMAX, OE and BJ, respectively. See [16] and [19] for model structures.

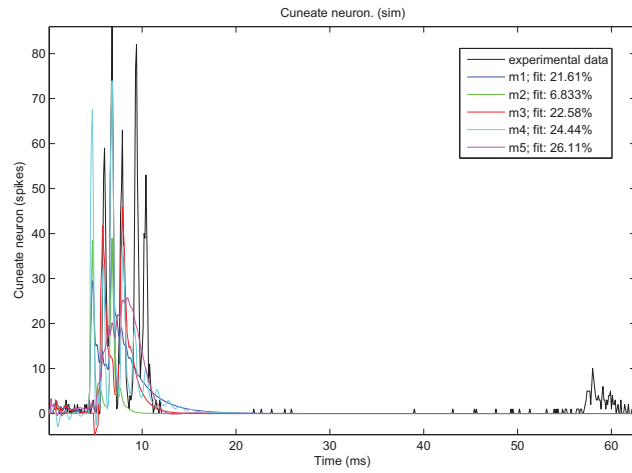


Figure 26: Models for the electrical stimulation for 0.1 ms bin width. Models m1-m5 are PEM, ARX, ARMAX, OE and BJ, respectively. See [16] and [19] for model structures.

4.1.3 Three Neuron Model: Tactile Stimulation

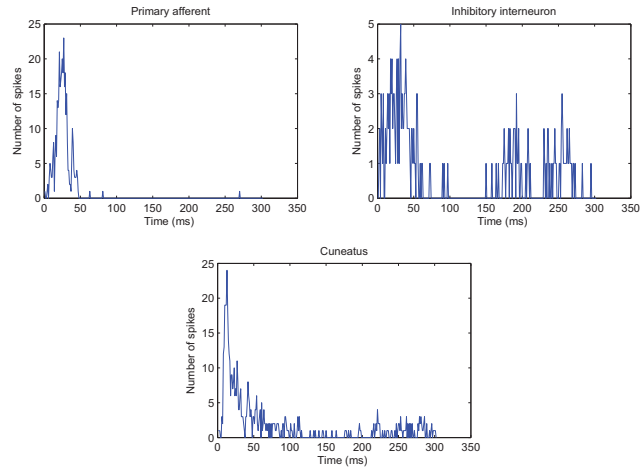


Figure 27: Experimental histogram data used for the two input single output modeling. The top diagrams show inputs from left to right: primary afferent and inhibitory interneuron, respectively. The lower diagram shows the output of the cuneate neuron. Data from [11].

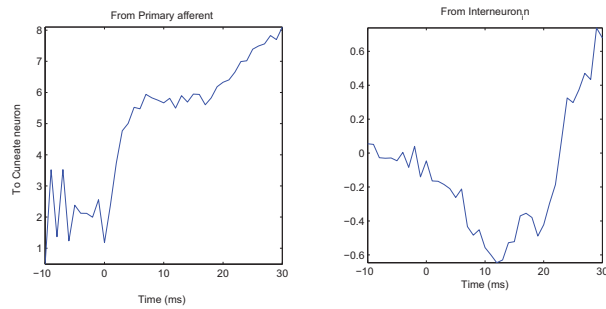


Figure 28: Cuneate neuron response to input step for the two input channels (primary afferent neuron and inhibitory interneuron). Data from [11].

The data used for the three neuron modeling is seen in Fig. 27. The interneuron data is unsmooth in relation to the others, as the number of experiments is small. This could potentially pose problems for the modeling. Step response for the same system is seen in Fig. 28. From this it is clear that the primary afferent neuron has an activating influence on the cuneate neuron and that the interneuron inhibits the cuneate neuron (as should be expected). The model ability to replicate the cuneate neuron output signal is seen in Fig. 29. In general, the fit of the models is slightly better than for the two neuron model. Also, what the models now are able to do is to take into account

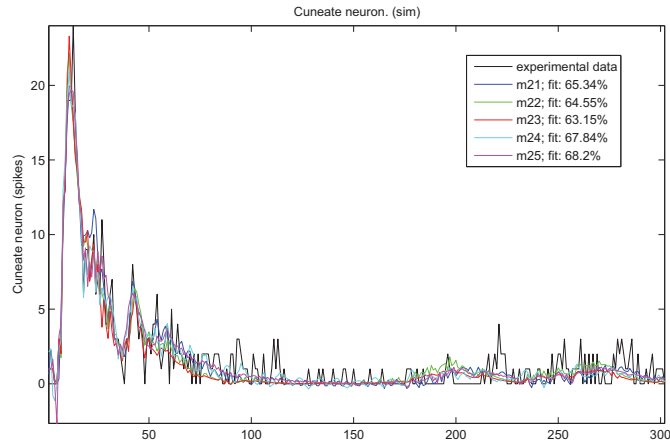


Figure 29: Modeling results for the two input (primary afferent and inhibitory interneuron) one output (cuneate neuron) three neuron model. Models m21-m25 are PEM, ARX, ARMAX, OE and BJ, respectively. The models are able to follow the signal better than the two neuron model, for the same cuneate neuron output. Especially the return of background activity is captured in this model, which is not seen in the two neuron model. Fit ranges between 64% and 70%. See [16] and [19] for model structures.

the return of the spontaneous activity of the cuneate neuron, far from the actual stimulation. Models are as previously PEM, ARX, ARMAX, OE, BJ and N4SID.

The different models are able to cover aspects of the system differently. Fig. 30 shows the bode diagram for the PEM model. Interesting aspects of this plot is that the model shows slightly differentiating properties and has phase lead, for a large part of the spectrum.

Fig. 31 shows the residual autocorrelation and cross correlation for two input single output PEM model, with 99%-confidence interval limits for noncorrelated residuals. This indicates that model m21 of order 6 can be accepted.

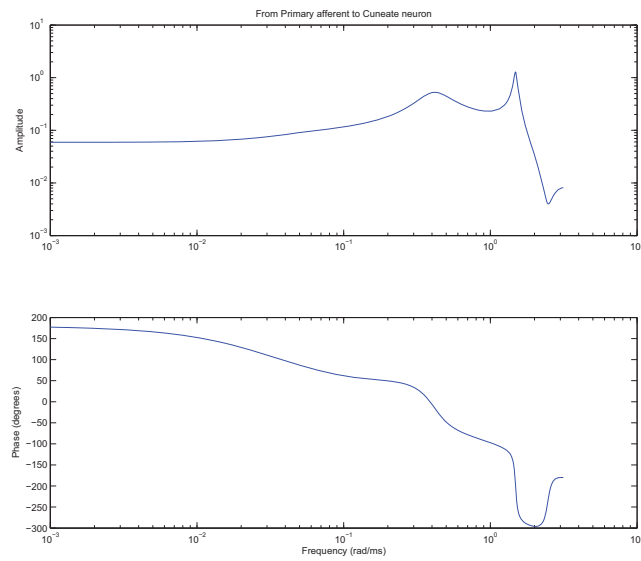


Figure 30: Bode diagram of the PEM model for the three neuron circuit. It is worth noting that the firing frequency of the primary afferent neurons never exceeds 500 Hz ($\simeq 10^{-1}$ rad/ms.)

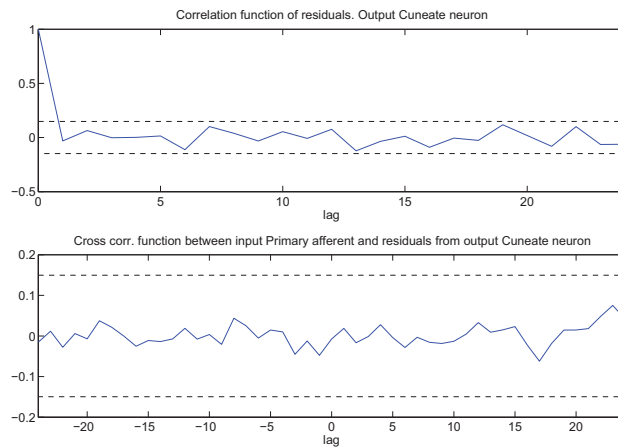


Figure 31: Residual autocorrelation (top) and cross correlation (bottom) for two input single output PEM model m21 of order 6 with 99%-confidence interval limits (dashed line) for noncorrelated residuals.

4.2 GESS Neuron Model

GESS: Generic Executable Stochastic Spiking neuron model v.2

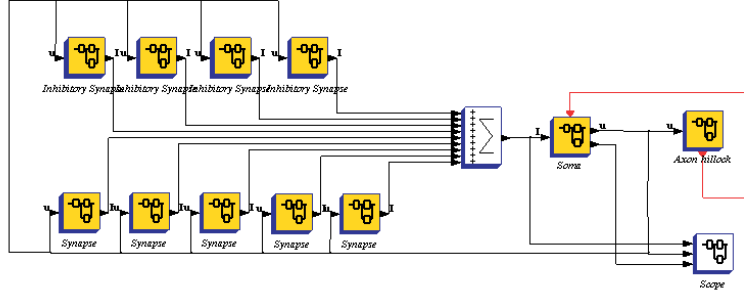


Figure 32: The modified GESS model created during this thesis. Compare to original block in Fig. 3. Aside from many changes in the superblocks, seen here are five excitatory synapses (lower left) and four inhibitory synapses (upper left).

An overview of the modified GESS cuneate neuron model, created during this thesis, is seen in Fig. 32. Seen here are five excitatory synapses and four inhibitory synapses. Each of these are fed with unique experimental spike-time data from a tactile stimulation. But in order to read data, a read data block was made, as seen in Fig. 33, replacing the block in Fig. 6. It is constructed in a way such that an event clock keeps track of time through a counter block. For each time, the input file is read, and if the time of the read line is lower than the clock the else block triggers a normalized action potential to be fired, of 1 ms duration. If not, the clock moves to the next time step (1 ms), gives 0 as output signal, and reads the input line again.

A block for generating an action potential when the cuneate neuron model fires spikes itself is identical to the one seen in Fig. 6. The block receives input from a block generating a spike event based on the membrane potential with some stochasticity, in the axon hillock.

The various constants were determined, by fitting model output with experimental data, to best recreate the cuneate neuron behavior, and can be seen in Table 1. Here, and for the duration of the GESS modeling, the cuneate neuron membrane resting potential has been moved from -50 mV to 0. The synapse scaled reversal potentials have also been scaled accordingly.

Fig. 34 shows one simulation of the GESS cuneate neuron model. The top diagram shows the net current flowing through the membrane, the middle diagram them membrande potential and the lower diagram the spike firing of the cuneate neuron.

The block for the Paired Pulse Depression (PPD) is seen in the top part of Figure 35. It modulates the gain g of the EPSP (Excitatory Post-Spike Potential) according to each interval t_{int} between two spikes in the following

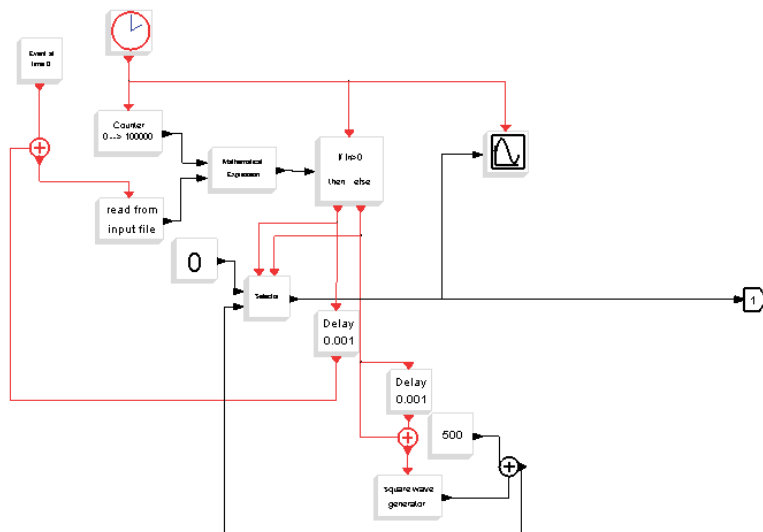


Figure 33: The read data block for the synapse of the neuron model created during this thesis. Compare to the original block in Fig. 6. The data (input file) is read for each clock-generated time. For each given time in the input file, a standardized action potential of 1 ms duration is generated, exported at (1). This replaces the block in Fig. 6. This block is used in the simulation resulting in Fig. 34

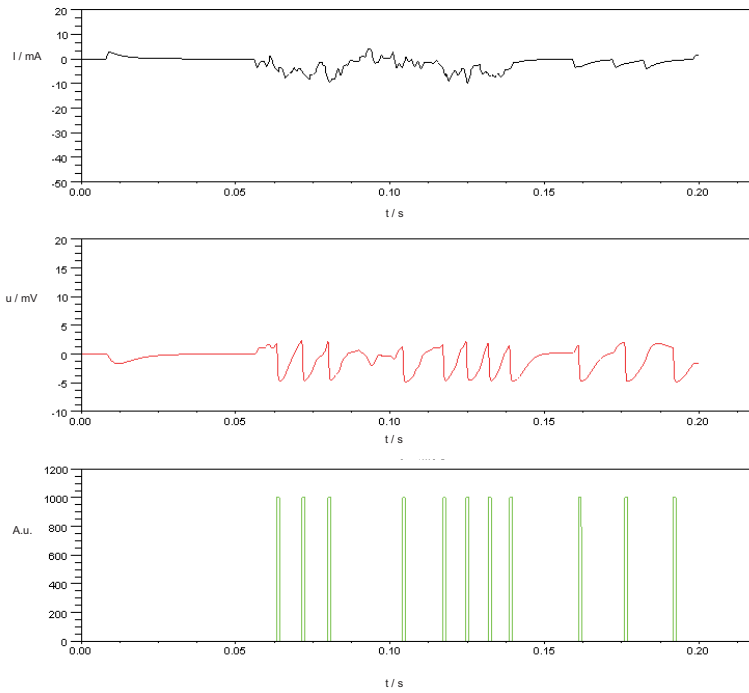


Figure 34: The output of the cuneate neuron model created during this thesis (Fig. 32) for tactile light touch stimulation, starting at 50 ms. The model is fed with single neuron experimental data for five excitatory and four inhibitory neurons. The top diagram shows the net current I flowing through the membrane, the middle diagram shows the membrane potential u and the lower diagram the spike firing activity of the cuneate neuron model versus time (s).

Table 1: Constants for the adjusted GESS model. The membrane resting potential is adjusted to 0 mV (from -50 mV according to ongoing work), and the excitatory and inhibitory synapse scaled reversal potentials are scaled accordingly.

<i>Constant</i>	<i>Value</i>	<i>Unit</i>
Excitatory synapse scaled reversal potential	50	<i>mV</i>
Excitatory synapse time constant τ	0.005	s^{-1}
Excitatory synapse gain g	0.0004	
Inhibitory synapse scaled reversal potential	-20	<i>mV</i>
Inhibitory synapse time constant τ	0.005	s^{-1}
Inhibitory synapse gain g	0.003	
Soma membrane time constant T	0.0025	<i>s</i>
Post-spike scaled reversal potential	-5	<i>mV</i>
Post-spike time constant τ	0.001	s^{-1}
Post-spike gain g	0.05	
Axon hillock absolute refractory period	0.001	<i>s</i>
Axon hillock offset	0	<i>mV</i>
Spiking intensity α	3	
Spiking intensity β	3.1	$(mV)^{-1}$
PPD time constant τ_{PPD}	0.005	s^{-1}

way:

$$g_{mod} = g \cdot \left(1 - e^{-\frac{t_{int}}{\tau_{PPD}}}\right) \quad (6)$$

The interspike interval CDF, ranging between 0 and 1, determines with the help of a random number between 0 and 1 the probability for spike discharge, according to

$$F = 1 - e^{-\int_0^t \alpha \cdot e^{\beta \cdot u}} \quad (7)$$

Where α and β are adjustable constants, dependent on membrane and synapse characteristics.

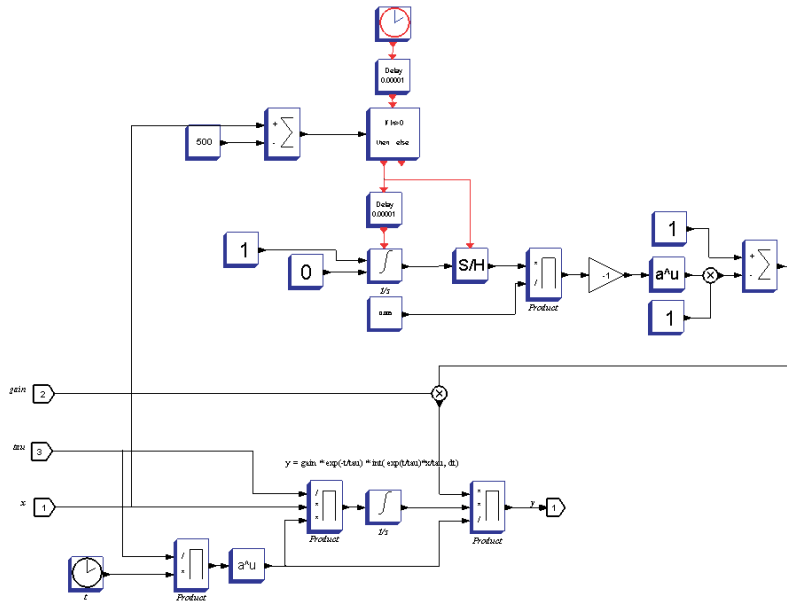


Figure 35: Superblock of the Paired Pulse Depression (PPD) unit (top), created during this thesis, as well as the unit for converting changing membrane potential in the synapse to net current (bottom, compare to the original block in Fig. 7). For each incoming action potential, the PPD unit (top) modifies the synapse gain g according to Eqn. 6, resulting in a reduced gain g as the interspike interval t_{int} decreases. A limitation is that the interspike interval t_{int} is measured as the difference in time between the current and previous action potential, unphysiologically not taking into account incoming action potentials before that.

5 Discussion

This thesis deals with the modeling and identification of the human movement control system in general, which involves the cerebellum and some other subunits of the nervous system, and the cuneate nucleus in particular. In order to build an understanding and a closed loop feedback system of human movement control, I chose to start by analyzing and understanding one subcomponent of the system. The anatomical architecture of the system is, by now, fairly well characterized. The question is how each subunit contributes to system behavior to produce movement control. To solve this, we started by looking at the cuneate nucleus, with hopes of being able to work our way into the cerebellum and back out again, cell type/subsystem by cell type/subsystem. This was not achieved in this thesis, and likely requires substantial effort beyond the scope of a single thesis like this one. However, a fair amount of work was put into trying to understand our starting block for this system: the cuneate nucleus.

In order to achieve stable movement control in general, a system needs feedback not only of the position x , but also of the speed \dot{x} of the controlled object. This can be achieved by having two different feedback signals x and \dot{x} or just one signal x , which can be differentiated to yield \dot{x} . It is believed that the muscle spindles transmit a linear combination of x and \dot{x} , whereas the primary afferent neurons only transmit information of the position x . It is thus necessary to differentiate this signal somewhere in the central nervous system in order to achieve stable movement control. A too strong feedback of the position x gives an oscillating error behavior, whereas a too weak feedback gives a persistent error. On the other hand, a too strong feedback of the speed \dot{x} could give a slow control whereas a too weak feedback could give rise to oscillations.

Another important aspect of a control system in general, and human movement control in particular, is adaptation and adaptive control. Control systems are often designed to have one loop being the controller for the system. Then, an outer loop controls the controller in an adaptive way, to compensate for internal errors in the control loop itself. Looking at Fig. 2, it is not far fetched to interpret the outer loop as being the control loop for the system, and the inner loop, including the lateral reticular nucleus, the inferior olive and the climbing fibres, as the adaptive part of human movement control. This is also where adaptation occurs *in vivo*, according to unpublished experimental data.

The cuneate nucleus accepts sensory information through primary afferent fibers, and modulates this. In the thesis a two pronged approach was used to understand this process. System modeling and identification of detailed experimental data, using MATLAB, yielded a number of models, some of which showed interesting characteristics such as phase lead and differentiation. These are interesting features from a control point of view, as this could improve the use of the input signal for motor control. However, not all models showed this.

There are many possible sources of error in this setup imposing limitations as to the conclusions that can be drawn. Starting with how the experiments are conducted, measuring repeatedly from one neuron instead of collecting data simultaneously from many input neurons, as well as the output from the cuneate neuron itself, leads to a problem of causality. Additionally, adding several consecutive stimulations into spike-time histograms incur an error as, for the tactile stimulation, the stimuli are not identical. Rather, similar stimuli are selected based on stimulation length. Using spike-time histograms, it is not far-fetched

to interpret these as probability density functions for action potential discharge. Selecting the action potentials using a pattern recognition software on the raw voltage data also leads to the possibility of errors. However, this error is likely small. The fact that the models behave quite differently leads to an assumption that the model error can in fact be quite large. Difficulties arise already when trying to incorporate the cuneate neuron background firing, which is an important feature of the cuneate neuron. It is reasonable to believe that the models need further validation before conclusions can be drawn with any certainty. This can be done using more experimental data of the same type and using different stimuli, for example.

The second approach to building a detailed understanding of the cuneate nucleus was done based on GESS, a program made by Henrik Jörntell and Martin Nilsson in 2008 [18]. A number of modifications to this were made, in order to make it behave like a cuneate neuron. The model now accepts experimental data as input and is, to a degree, able to give an output much like experimental output data is. There are several limitations and sources of error in this model. Regarding the experimental data, similar errors as for the Matlab models are to be expected. However, spike time histograms are not used here. The number of simulated synapses is too low forcing high individual synapse gain, likely adding significant errors to simulation output since individual primary afferent fibers can have too high an impact. Using only 1 ms time resolution can be a major problem for fast firing neurons, such as the cuneate neuron, limiting the maximum firing frequency and failing to realize fast changes in neuron current and membrane potential. A problem the original model also had was the fact that the individual synapses are affected by the global membrane potential only, not including membrane conductance. This is a problem when many synapses are activated simultaneously.

This work is only one starting point; much work still needs to be done in order to answer these questions, and to get a system understanding of how movement control is achieved. The work was explorative in nature, and it has at times been difficult to know the best way forth, due to my own inexperience in the field of neuroscience and automatic control, and due to the fact that this is unexplored terrain. Henrik Jörntell and Rolf Johansson have, however, given many helpful insights along the way.

However, assuming the primary afferent fibres only transmit information of the position x , and assuming our models are correct, this indicates that the cuneate nucleus acts as a differentiating filter of the afferent sensory signal necessary to achieve good movement control. This does not exclude other parts of the central nervous system from doing the same, but could shed light on the importance of the cuneate nucleus in human movement control. Using similar strategies as was used in this work, further work could include analyzing other parts of what is believed to be important structures for human movement control, *e.g.* as seen in Fig. 2. When these pieces are then put together, this could then help to build a control system understanding of human movement control which could be of great interest to neurophysiologists and people with interest in automatic control in general. It does not need to stop there, however, as the cerebellum is believed to be involved in not only movement control, but other sorts of control as well, such as the control of higher mental functions in the cerebrum including thought processes.

6 Conclusion

Our preliminary findings suggest that system identification can be used to identify the mathematical properties of a local neural structure with an uncomplicated network structure. Based on these findings and the previous experimental work by Jörntell and Bengtsson, further modeling of neural structures in and outside the cerebellum in order to build a control system understanding, could potentially give new insights into cerebellar movement control. This, how the cerebellum achieves movement control, could be of great interest not only in the field of neuroscience, but in robotics and other control applications as well.

Acknowledgements

I would like to thank Henrik Jörntell and Rolf Johansson for valuable support throughout this thesis. In particular, I would like to thank Henrik for warmly welcoming me, allowing me to work at the department of cerebellar physiology and for helping me both with practical and theoretical aspects of this thesis on a day-to-day basis. I would like to thank Rolf for introducing me to this field, and for many helpful insights and valuable support throughout the thesis. I would like to thank the others at the department of cerebellar physiology (Fredrik Bengtsson, Carl-Fredrik Ekeröth and Kersti Larsson) for a fun and inspiring work environment, as well as the rest of people at the section for neurophysiology at the medical faculty at Lund University. I would also like to thank Jonas Dürango for inspiring discussions and helpful comments since he's joined. My family and Lotta deserve special thanks for always being there, always supportive and always loving. Finally I would thank my savior and my all, Jesus Christ. To God be the glory, forever and ever.

A Modeling details

Below is the PEM model used for the MATLAB two neuron modeling, referred to as m1.

$$\begin{aligned} \text{State space model } x(t + Ts) &= Ax(t) + Bu(t) + Ke(t) \\ y(t) &= Cx(t) + Du(t) + e(t) \end{aligned}$$

$$A = \begin{bmatrix} 1.0281 & 0.1103 & -0.0329 & -0.0179 & -0.0476 \\ 0.0078 & 0.9167 & 0.1257 & -0.0376 & 0.5252 \\ -0.0744 & -0.0056 & 0.8474 & 0.3213 & -0.0070 \\ -0.0002 & -0.0528 & -0.4983 & 0.7843 & 0.0813 \\ -0.0207 & -0.1959 & -0.0113 & -0.3575 & 0.7903 \end{bmatrix}$$

$$B = \begin{bmatrix} 0.0027 \\ -0.0163 \\ -0.0004 \\ -0.0095 \\ 0.0018 \end{bmatrix}$$

$$C = [20.5466 \quad -9.6495 \quad 4.4225 \quad 1.8089 \quad 5.8488]$$

$$D = 0$$

$$K = \begin{bmatrix} 0.0026 \\ 0.0022 \\ 0.0033 \\ 0.0070 \\ -0.0039 \end{bmatrix}$$

$$x(0) = \begin{bmatrix} 0.1533 \\ 0.1466 \\ -0.2072 \\ -0.7240 \\ 0.2806 \end{bmatrix}$$

Loss function 0.996014 and FPE 1.12794, sampling interval: 1 ms

Below is the PEM model used for the MATLAB three neuron modeling, referred to as m21.

$$\begin{aligned} \text{State space model } x(t + Ts) &= Ax(t) + Bu(t) + Ke(t) \\ y(t) &= Cx(t) + Du(t) + e(t) \end{aligned}$$

$$A = \begin{bmatrix} 1.0258 & -0.0233 & 0.1858 & 0.2434 & -0.0873 & -0.1290 \\ -0.1628 & 0.7139 & -0.4489 & -0.2434 & 0.0616 & -0.2960 \\ 0.0722 & 0.2712 & 0.8782 & 0.0375 & 0.3800 & -0.2178 \\ -0.0376 & 0.2230 & 0.3693 & -0.4453 & -0.8747 & 0.2132 \\ 0.0270 & -0.1280 & -0.0218 & 0.5497 & -0.2056 & -0.6874 \\ 0.0084 & -0.0805 & 0.0072 & -0.8525 & 0.2864 & -0.4879 \end{bmatrix}$$

$$B = \begin{bmatrix} 0.0046 & 0.0341 \\ -0.0009 & 0.0093 \\ -0.0002 & -0.0358 \\ -0.0104 & -0.0612 \\ 0.0053 & 0.0656 \\ 0.0146 & 0.0199 \end{bmatrix}$$

$$C = \begin{bmatrix} 17.4587 & -7.2585 & 1.7610 & -0.3637 & 6.5012 & 3.1413 \\ 3.6317 & 3.3660 & 2.5861 & 0.4609 & 0.9220 & 2.2538 \end{bmatrix}$$

$$D = \begin{bmatrix} 0 & 0 \\ 0 & 0 \end{bmatrix}$$

$$K = \begin{bmatrix} 0.0030 \\ -0.0058 \\ -0.0006 \\ 0.0106 \\ -0.0009 \\ 0.0057 \end{bmatrix}$$

$$x(0) = \begin{bmatrix} 0.4389 \\ -0.6503 \\ 0.9078 \\ -0.7040 \\ 0.4908 \\ 0.6128 \end{bmatrix}$$

Loss function 0.906593 and FPE 1.08671; Sampling interval: 1 ms

References

- [1] Ito, M. Cerebellar circuitry as a neuronal machine. *Progress in Neurobiology* **78**, 272-303 (2006)
- [2] Apps, R & Garwicz, M. Anatomical and physiological foundations of cerebellar information processing. *Neuroscience* **6**, 297-311 (2005)
- [3] Wolpert, D. M., Miall R. C. & Kawato, M. Internal models in the cerebellum. *Trends in Cognitive Sciences* **2**, 338-347 (1998)
- [4] Burdet, E., Tee, K. P., Mareels, I., Milner, T. E., Chew, C. M., Franklin, D. W., Osu, R. & Kawato, M. Stability and motor adaptation in human arm movements. *Biological Cybernetics* **94**, 20-32 (2006)
- [5] Doya, K., Kimura, H. & Kawato, M. Neural Mechanisms of Learning and Control. *IEEE Control Systems Magazine* 42-54 (2001)
- [6] Tien, J. H. & Guckenheimer, J. Parameter estimation for bursting neural models. *Journal of Computational Neuroscience* **24** 358-373 (2008)
- [7] Brette, R., Rudolph, M., Crnevale, T., Hines, M., Beeman, D., Bower, J. M., Diesmann, M., Morrison, A., Goodman, P. H., Harris, F. C., Zirpe, M., Natschläger, T., Pecevski, D., Ermentrout, B., Djurfeldt, M., Lansner, A., Rochel, O., Vieville, T., Muller, E., Davidson, A. P., Boustani, S. E. & Destexhe, A. Simulation of networks of spiking neurons: A review of tools and strategies. *Journal of Computational Neuroscience* **23**:349-398 (2007)
- [8] Ferrington, D. G., Rowe, M. J. & Tarvin, R. P. C. Actions of single sensory fibres on cat dorsal column nuclei neurones: vibratory signalling in a one-to-one linkage. *Journal of Physiology* **386** 293-309 (1986)
- [9] Coleman, T. G., Zhang, H-Q. & Rowe, M. J. Transmission Security for Single Kinesthetic Afferent Fibers of Joint Origin and Their Target Cuneate Neurons in the Cat. *The Journal of Neuroscience* **23(7)** 2980-2992 (2003)
- [10] Rasmusson, D. D. & Northgrave, S. A. Reorganization of the Raccoon Cuneate Nucleus After Peripheral Denervation. *The Journal of Neurophysiology* **78** 2924-2938 (1997)
- [11] Bengtsson, B. & Jörntell, H. Sensory transmission in cerebellar granule cells relies on similarly coded mossy fiber inputs. *PNAS* **106**, 2389-2394 (2009).
- [12] Jörntell, H. & Ekerot, C-F. Receptive Field Plasticity Profoundly Alters the Cutaneous Parallel Fiber Synaptic Input to Cerebellar Interneurons. *The Journal of Neuroscience* **23(29)** 9620-9631 (2003)
- [13] Jörntell, H. & Hansel, C. Synaptic Memories Upside Down: Bidirectional Plasticity at Cerebellar Parallel Fiber-Purkinje Cell Synapses *In Vivo*. *Neuron* **52** 227-238 (2006)
- [14] Jörntell, H. & Ekerot, C-F. Properties of Somatosensory Synaptic Integration in Cerebellar Granule Cells *In Vivo*. *The Journal of Neuroscience* **26(45)** 11786-11797 (2006)
- [15] Jörntell, H. & Ekerot, C-F. Reciprocal Bidirectional Plasticity of Parallel Fiber Receptive Fields in Cerebellar Purkinje Cells and Their Afferent Interneurons. *Neuron* **34** 797-806 (2002)
- [16] Johansson, R. System Modeling & Identification. *Prentice Hall*, Englewood Cliffs, NJ 1993; Spring 2009 *Rev. Edition*, Lund, 2009
- [17] <http://www.scicoslab.org/>
- [18] <http://www.osf.org> [OSF 2008] 2008-07-12
- [19] Ljung, L. System Identification ToolboxTM 7 User's Guide. *The MathWorks*, Natick, MA; September 2009